A UDE-based Controller with Targeted Filtering for the Stabilization of a Fixed-Wing UAV in the Harrier Maneuver

Pravin Wedage
Institute for Aerospace Studies
University of Toronto
pravin.wedage@flight.utias.utoronto.ca

Hugh H.-T. Liu
Institute for Aerospace Studies
University of Toronto
hugh.liu@utoronto.ca

***Abstract*— Autonomous aerobatic flight for fixed-wing aerial vehicles is studied. This paper proposes an uncertainty and disturbance estimator (UDE) based controller that attenuates the special effect of model uncertainty and external disturbances during the aerobatic harrier maneuver using a novel targeted filtering structure. Knowledge of the disturbance frequency content and the undisturbed system dynamics are used in filter design to improve disturbance rejection compared with standard UDE-based controllers with low-pass filtering structures. The controller performance is validated on a simulated model of a vehicle performing the low-speed, high angle-of-attack harrier aerobatic maneuver.**

I. Introduction

recent years, modern UAV systems have become increasingly popular for a growing number of applications in both industry and academia. This increasing demand has led to a variety of efforts to increase the operating capabilities through various means, such as novel configurations and improved controllers. One such area of focus is the development of aerobatic maneuvering controllers for fixed-wing vehicles, in order to expand their low-speed, close-quarters maneuverability. When compared with quadrotor platforms, standard fixed-wing UAS do not have the same maneuvering capabilities at or near hover, due to their inherent airfoil-type lifting and control surfaces. As a result, the use of fixed-wing vehicles in small, closed, or cluttered areas such as indoor spaces or cluttered environments is heavily restricted. However, fixed-wing vehicles have far greater range and endurance capabilities, and efforts to expand their maneuvering capabilities have been undertaken in order to produce a vehicle platform with both range and close-quarters maneuverability. Of these novel design efforts, controllers designed to enable aerobatic, post-stall maneuvering for fixed-wing vehicles have been shown to be promising for improving the maneuverability of fixed-wings without modifying the typical control surface arrangement of the vehicle [1]–[6]. Aerobatic maneuvering enables fixed-wing vehicles to travel at very low airspeeds, even hovering like a quadrotor, and also allows for extremely low radius turns, compared to a non-maneuvering vehicle. The result is a greatly enhanced operating envelope for fixed-wing vehicles, which enables their use indoors and in tight or obstacle-rich environments [1], [7]. The focus of this paper is the design and development of an Uncertainty and Disturbance Estimator (UDE) based controller that is capable of stabilizing the harrier aerobatic maneuver. A novel filtering structure for UDE controllers is introduced, which uses targeted filtering to attenuate the effects of disturbances better than conventional UDE filtering structures.

Aerobatic maneuvering itself for fixed-wing vehicles generally consists of maneuvers that involve quick/continuous rotations, high angle-of-attack/sideslip, and/or low airspeeds. These conditions introduce significant nonlinearities to the aircraft dynamics, and the behaviour departs significantly from aircraft in a non-aerobatic maneuvering case [8]–[12]. The principal factor in the nonlinear response is the high angle-of-attack, which induces stall over many of the aircraft lifting surfaces. The resulting lift and drag response over these surfaces is not only highly nonlinear, but subject to time-varying effects such as vortex shedding due to the complex separated flow behind the stalled wings. Ordinarily, a fixed-wing vehicle would struggle to maintain lift, but aerobatic fixed-wing vehicles have high thrust-to-weight ratios, with strong propellers that can support the vehicle and also provide additional airflow that allows the control surfaces to remain unstalled. The challenge with designing controllers for aerobatic maneuvering is the lack of aerodynamic data; a great deal of data would be required to model the full flight envelope, and very little experimental data is available for the Reynold's number typical for these vehicles ($R_e < 10^6$). Even if the physical effects acting on a vehicle can be modelled, the simulated result may deviate significantly from the real system. In order to address the impact of these unknown nonlinearities, model uncertainties and other disturbances, an Uncertainty and Disturbance Estimator based robust controller is implemented in order to estimate their combined effect as a lumped disturbance term.

UDE-based controllers have been used in various applications where there have been complex or difficult to model disturbances [13]–[16]. In general, UDE is a combination of a baseline controller for the "undisturbed" system and a filtered disturbance estimate component. Regarding disturbances, UDE can treat modelling uncertainties, unknown dynamics, and disturbances with a combined estimation structure that only requires the frequency information of the lumped disturbances, compared to other disturbance estimation schemes such as ADRC, DOBC, or EID that require additional constraints on or knowledge of the distubances or the plant model [17]. This makes UDE an excellent

choice for addressing the post-stall nonlinearities and lack of aerodynamic data in this application. Two cases of successful application of UDE are relevant: in Zhang [14], a UDE-based controller was used to stabilize the position of fixed-wing vehicles optimally in the presence of disturbances caused by the trailing vortices of the leading vehicle, and in Kuperman [15], a UDE-based controller was applied to stabilize nonlinear roll oscillations during high angle of attack flight on a simplified linear model.

The main contribution of this paper is the development of a novel UDE-based controller with targeted filtering that attenuates the effect of disturbances on tracking error more strongly, compared to previous UDE controllers. For verification, the low airspeed, high angle-of-attack, harrier maneuver is chosen as a representative maneuver; this maneuver allows the vehicle to travel below cruise stall speed with a large pitch angle, directly resulting in a significantly reduced takeoff distance. It can be performed without using a robust controller, but implementations often result in significant trajectory tracking error [5], [7]. The structure of this paper is as follows: Section II details the aircraft model and nonlinear behaviour, Section III details the UDE controller structure and novel filtering design methodology, with simulation results presented in Section IV.

II. Aircraft Modelling

To test the proposed controller, an aircraft model was developed with the goal of representing the key features of the aircraft dynamics that affect aerobatic maneuvering. The majority of these effects are related to the high angle-of-attack and the propwash, which are the two critical features of aerobatic maneuvering. Due to the complexity of post-stall dynamics, it is expected that there will still be discrepancies between the modelled dynamics and the real system; however, the goal is to develop a model that captures the main features of the maneuvering vehicle. This section also serves to highlight key features of the vehicle dynamics, which directly relate to the applicability of the control law.

The aircraft is modelled in simulation using standard 6DOF dynamic equations [18]. However, the computation of the forces and moments becomes more complex, for several reasons. First, due to the high angle-of-attack, the forces and moments acting on the aircraft surfaces are well outside the linear range with respect to angle of attack. Second, it is necessary to be able to account for differing dynamic pressures along different components of the vehicle, due to the varying local velocities across the lifting surfaces that occur because of aircraft geometry and strong propwash flow over some surfaces. To address these needs, the component breakdown approach or strip theory approach is used, which computes the total force and moment on the aircraft by summation of the forces and moments acting on individual components about the center of gravity [8], [9]:

$$\boldsymbol{F} = \sum_{i=1}^{N} \boldsymbol{F}_i \tag{1}$$

$$\boldsymbol{M} = \sum_{i=1}^{N} \boldsymbol{M}_{i,ac} + \sum_{i=1}^{N} \boldsymbol{r}_i \times \boldsymbol{F}_i \tag{2}$$

The components themselves can be thought of as elements of each aircraft surface. The boundaries between these elements align on the physical boundaries (ex. control surfaces) as well as locations where there are large differences in the local flow (ex. inside and outside of the propwash). The forces and moments for each section can be computed as follows:

$$\boldsymbol{F}_i = \frac{1}{2}\rho V_i^2 S_i \begin{bmatrix} C_X(\alpha_i, \beta_i) \\ C_Y(\alpha_i, \beta_i) \\ C_Z(\alpha_i, \beta_i) \end{bmatrix} \tag{3}$$

$$\boldsymbol{M}_{i,ac} = \frac{1}{2}\rho V_i^2 S_i \begin{bmatrix} 0 \\ c_i C_m(\alpha_i, \beta_i) \\ 0 \end{bmatrix} \tag{4}$$

where V_i is the magnitude of the local velocity over section i, S_i is wetted area for the element, α_i and β_i are the local angle-of-attack and sideslip angle, and $\boldsymbol{R_i}$ is the orientation of section i relative to the local incoming airflow. However, note that the local velocity V_i is not only the free-stream velocity, but a combination of the freestream velocity V_∞, induced propwash velocity V_{ind}, and the induced velocity from other wing sections:

$$V_i = V_{\infty,i} + V_{ind,i} + \sum_{j=1}^{N} \frac{\Gamma_j}{\bar{c}_j} v_{ji} \tag{5}$$

In order to compute this velocity as well as the local aerodynamic angles, a nonlinear-lifting line code is applied. A nonlinear relation between the circulation Γ of the horseshoe vortex around a wing location i and the lift response at that section can be obtained, leading to a system of nonlinear equations that can be used to solve for the circulations:

$$\rho \Gamma_i \left(V_i\right) \times d\ell_i - \frac{1}{2}\rho ||V_i||^2 C_{L_i}(\alpha_i, \delta_i) dA_i = 0 \tag{6}$$

v_{ji} is the dimensionless induced velocity of vortex j at a location on vortex i, obtained using the Biot-Savart law, $d\ell_i$ is the length of the bound section of vortex i, and dA_i is the wing area represented by vortex i. Originally, the lifting line method was developed by Prandtl for unswept, high aspect-ratio wings in the linear lift regime, but the modern modifications have found it to be suitable for the low-Reynolds, high angle-of-attack flow that occurs during the harrier maneuver [19], [20].

The nondimensional coefficients C_X, C_Y, C_Z are of critical importance, as they contain the majority of information about the aerodynamic response especially at high angle-of-attack. For the post-stall range of angle-of-attack that the vehicle experiences during maneuvering, a complex relationship exists between the angle-of-attack and the system

response, and typical simulation efforts utilize lookup tables based on experimental data captured at appropriate Reynold's number flow conditions. Though the coefficient responses can resemble sinusoidal functions, the response is complex and highly nonlinear just beyond the stall angle-of-attack, with a pronounced departure from the linear lift regime [9], [10]. For this work, the aerodynamic data is obtained through a data-fusion process combining XFLR5 predictions and experimental data [9], [21].

The propwash is a core component of the dynamic model, as this propeller induced flow is what enables the vehicle to successfully perform the harrier maneuver. The goal is to ensure it is modelled well enough to reflect its actual influence on the vehicle. The approach utilized follows the method described in [22], which uses momentum theory to compute the induced velocity [23]:

$$V_{ind} = \frac{1}{2} k_w \left[-V_\infty + \sqrt{V_\infty^2 + \frac{2T}{\rho A}} \right] \tag{7}$$

V_{ind} is the downstream induced velocity, k_w is a load factor parameter dependent on the ratio between freestream velocity V_∞ and the velocity at the propeller disc, A is the propeller disc area, and T is the propeller thrust. The thrust and torque of the propeller are computed with blade element momentum theory, with some additional considerations involving propeller angle-of-attack. The area of effect of the propwash is assumed to envelope the entire tail, and some portions of the main wing based on aircraft velocity. The effects of flow shielding, vehicle rotation and downwash on the induced propwash velocity are also accounted for [9], [22].

The final component of the modelling structure is the time-varying components of the flow, which directly influence the UDE-based control design. Two main components are captured: first, the fluctuating airspeed generated by wind turbulence, and second, a time-varying change in lift and drag coefficients due to vortex shedding during stall. The wind turbulence can be easily implemented using the von Karman model [24]. The vortex shedding effect is implemented using experimental data, and has been measured to cause up to a 40% change in magnitude for the aerodynamic coefficients [25]–[27]. The inclusion of these effects results in time-varying disturbances acting upon the vehicle model, whose frequency characteristics are utilized in this paper to improve disturbance estimation and reduce tracking error. In the simulation, vortex shedding is applied directly to the lift and drag coefficients as follows:

$$C_L' = C_L(\alpha, \delta) + \lambda_{vs} \sin(2\pi f_{vs} t + \phi_r) \tag{8}$$

where λ_{vs} is a gain function that is nonzero only beyond a critical angle-of-attack, f_{vs} is the frequency of vortex shedding, and ϕ_r is a random introduced phase. The frequency of the vortex shedding phenomenon is obtained from experimental data [26], [27].

III. Control Architecture

A. General UDE Controller

In order to provide a robust control solution for the design problem, a UDE controller was developed in order address the uncertainties in aerodynamic modelling of the aircraft and disturbance effects experienced during aerobatic maneuvers. The UDE controller shown here is intended to be used for a system with a base linear controller, though UDE can augment nonlinear controllers as well. Consider a system with the following dynamics:

$$\dot{\boldsymbol{x}} = \boldsymbol{A}\boldsymbol{x} + \boldsymbol{B}\boldsymbol{u} + \boldsymbol{d} \tag{9}$$

where $\boldsymbol{x}, \boldsymbol{u}$ are the state and control vectors, $\boldsymbol{A}, \boldsymbol{B}$ are the state and control matrices, and $\boldsymbol{d}$ is a vector of lumped disturbances. The UDE control law is a combination of a linear control solution (ex. LQR) for the base undisturbed system with $\boldsymbol{d} = 0$, denoted as $\boldsymbol{u}_0$, and an additional component that compensates for the disturbances, $\boldsymbol{d}_e$. The disturbance component is a filtered estimate of the disturbances based on the system dynamics in (9). The general UDE control law can be presented as follows, based on previously derived UDE controllers and using LQR as a nominal controller [14], [15]:

$$\boldsymbol{B}\boldsymbol{u} = \boldsymbol{B}\boldsymbol{u}_0 - \boldsymbol{d}_e \tag{10}$$

$$\boldsymbol{B}\boldsymbol{u} = -\boldsymbol{B}\boldsymbol{K}\boldsymbol{x} - \boldsymbol{d}_e \tag{11}$$

A quick examination of the closed loop dynamics shows that the system will be stable if the base linear system is stable and the disturbance estimate converges to the disturbance.

$$\dot{\boldsymbol{x}} = (\boldsymbol{A} - \boldsymbol{B}\boldsymbol{K})\boldsymbol{x} + \boldsymbol{d} - \boldsymbol{d_e} \tag{12}$$

The above control law (11) will be expanded to present the explicit structure that is used in the harrier maneuver controller. The general control law (11) is substituted into the system dynamics (9), and an expression for the filtered disturbance estimate $\boldsymbol{d}_e$ using a filter $\boldsymbol{G}_f(s)$ can be obtained:

$$\boldsymbol{d}_e = \boldsymbol{G}_f(s)\boldsymbol{d} \tag{13}$$

$$\boldsymbol{d}_e = \boldsymbol{G}_f(s)(\dot{\boldsymbol{x}} - \boldsymbol{A}\boldsymbol{x} - \boldsymbol{B}\boldsymbol{u})$$

$$\boldsymbol{d}_e = \boldsymbol{G}_f(s)(\dot{\boldsymbol{x}} - \boldsymbol{A}\boldsymbol{x} - \boldsymbol{B}\boldsymbol{u}_0 + \boldsymbol{B}\boldsymbol{d}_e)$$

$$\boldsymbol{d}_e = \frac{\boldsymbol{G}_f(s)}{1 - \boldsymbol{G}_f(s)}(\dot{\boldsymbol{x}} - \boldsymbol{A}\boldsymbol{x} - \boldsymbol{B}\boldsymbol{u}_0) \tag{14}$$

The frequency domain control law can then be given by

$$\boldsymbol{u} = \boldsymbol{B}^+ \left(-\boldsymbol{B}\boldsymbol{K}\boldsymbol{x} - \frac{\boldsymbol{G}_f(s)}{1 - \boldsymbol{G}_f(s)} \left[\dot{\boldsymbol{x}} - (\boldsymbol{A} - \boldsymbol{B}\boldsymbol{K})\boldsymbol{x} \right] \right) \tag{15}$$

where $\boldsymbol{B}^+$ is the pseudo-inverse of $\boldsymbol{B}$, $\boldsymbol{B}^+ = (\boldsymbol{B}^{\boldsymbol{T}}\boldsymbol{B})^{-1}\boldsymbol{B}^T$, which exists if $(I - \boldsymbol{B}\boldsymbol{B}^+)$ is negligible.

Though the aircraft model has been described in Section II as highly nonlinear, the control structure with a linear reference model is believed to be suitable for the following reasons:

1) The majority of aircraft control surfaces are under linear flow regime due to the propeller wash that

envelopes the entire tail and the inboard sections of the main wing, even if the vehicle angle-of-attack is in the stall regime for non-maneuvering flight operations.
2) The lifting surfaces experiencing nonlinear stall phenomenon can be thought of as experiencing a linear combination of aerodynamic forces, where one component is the lift/drag under a linear assumption and the other is the change in lift and drag due to stall.

In other words, the disturbance estimator component will primarily estimate the additional lift due to propwash, and the effect of how stall causes the aircraft response to depart from its ordinarily quasi-linear response.

B. UDE Filter Design

The purpose of the novel UDE filter is to improve the disturbance rejection capabilities of UDE by improving the signal filtering and targeting specific known disturbances based on their frequency. This need is also reinforced by the performance and requirements of UDE in previous applications. A fundamental assumption in the standard UDE approach with a first-order low pass filter is that the cutoff frequency of filter greatly exceeds the frequency content of the disturbances, and in general, a higher cutoff frequency corresponds to better disturbance estimation. However, there is an upper limit on the frequency of this filter to prevent susceptibility to measurement noise and other uncertainty, which depends on the experimental application. As disturbance frequencies increase, the effectiveness of the low-pass filter in the UDE controller diminishes. However, it has been found that directly incorporating the system properties in the filter design process can lead to more effective disturbance rejection. The error dynamics of the closed-loop system in the frequency domain can be obtained by substituting the control law (15) into the system dynamics (9):

$$\begin{aligned} \boldsymbol{X}(s) &= -[s\boldsymbol{I} - (\boldsymbol{A} + \boldsymbol{B}\boldsymbol{K})]^{-1}(\boldsymbol{I} - \boldsymbol{G}_f(s))\boldsymbol{D}(s) \\ \boldsymbol{X}(s) &= -\boldsymbol{Z}(s)\boldsymbol{D}(s) \end{aligned} \tag{16}$$

The above structure implies that the proper design of $\boldsymbol{Z}(s)$ can lead to improved tracking performance, if $\boldsymbol{Z}(s)$ is small in the frequency range where $\boldsymbol{D}(s)$ is non-zero. Therefore, instead of focusing on designing only $\boldsymbol{G}_f(s)$ to improve capture and estimation of disturbances, the targeted filtering design method focuses on minimizing $\boldsymbol{Z}(s)$. The singular values of $\boldsymbol{Z}(s)$, treated as the gains the transfer function between the inputs $\boldsymbol{D}(s)$ and outputs $\boldsymbol{X}(s)$, can be used to evaluate the the filtering performance of the novel control law.

In typical UDE applications, $\boldsymbol{G}_f(s)$ is a low-pass filter:

$$\boldsymbol{G}_{f_{lp}}(s) = \frac{\omega_{lp}}{\omega_{lp} + s} \tag{17}$$

where ω_{lp} is the cutoff frequency in (rad/s). To improve disturbance estimation and rejection in this case, a novel filter composed of a combination of lower order filters is implemented:

$$\boldsymbol{G}_{f_n}(s) = \frac{2\omega_{lp}s + \omega_{lp}^2}{s^2 + 2\omega_{lp}s + \omega_{lp}^2} + K_{lp}\left(\frac{s^2 + \frac{\omega_{vs}}{Q_{vs}}\mu s}{s^3 + s^2 + \frac{\omega_{vs}}{Q_{vs}}s + \omega_{vs}^2}\right) \tag{18}$$

where $\omega_{lp}, K_{lp}, \omega_{vs}, Q_{vs}, \mu$ are design parameters of the filter. Though (18) can be represented as a single 5^{th} order filter, the form presented here offers some better insight. The first term is a general linear broad-spectrum filter, which by itself provides a marginal increase in performance compared to a low-pass filter. This term attenuates disturbances across a large frequency range below the cutoff frequency ω_{lp}. The second term is a third-order band-pass filter, which amplifies the disturbance signal in frequency range of interest. However, due to this additive structure and interaction with the first term, the pass-band of the combined filter (18) does not correspond to the pass-band of the second term. The Bode plots for magnitude and phase of the two filters (17) and (18) are presented in Fig. 1, where it can be seen that the frequency responses do not appear to vary significantly, in both magnitude and phase.

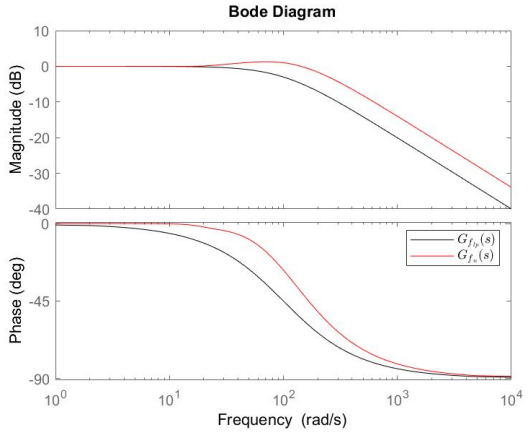

Fig. 1. Bode plots of the typical UDE low-pass filter (black) and the novel proposed filter (red).

With this targeted filtering structure, it is necessary to identify the frequencies for which $D(s)$ is non-zero. For a linear system, if the frequencies of particular time-varying effects are known, then the frequencies of the lumped disturbance term can be directly known. However, for the real system, this may not be the case, as there are highly nonlinear effects that are much more complex than the aerodynamic model can reasonably expect to predict. Therefore, to obtain a more accurate representation of the disturbance frequencies, the power spectral density of the system state variables during the aerobatic maneuver of interest is obtained. By using spectral density, the analysis of the disturbance frequencies is independent of any attempt at modelling the complex post-stall flow. During the harrier maneuver, the spectral density of the angle-of-attack is obtained. It can be seen in Fig. 2 that while there is high frequency range content in the signal, the majority of the disturbance content is in the low-frequency

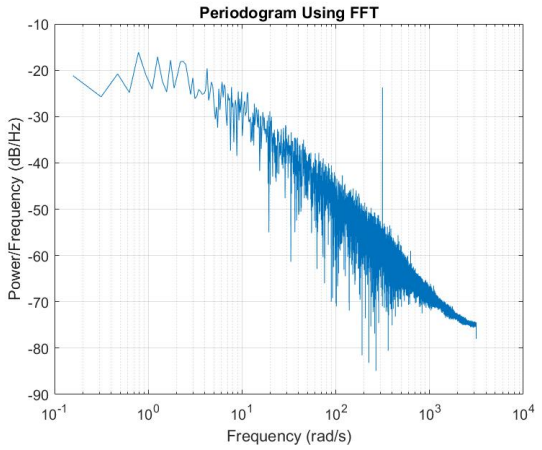

Fig. 2. Power spectral density of angle of attack for vehicle performing harrier maneuver at 45° .

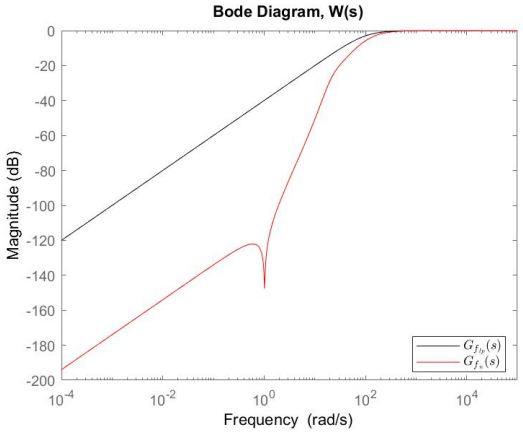

Fig. 3. Bode magnitude plot of the transfer function $\boldsymbol{W}(s)$, with the standard UDE low-pass filter (black) and the novel proposed filter (red).

range. Therefore, the design of $\boldsymbol{Z}(s)$ should modify $\boldsymbol{G}_{f_n}(s)$ for this particular range concentrated around 1 rad/s.

The stability characteristics of the controller can be determined by examining the properties of the filter. It is trivial to show that the undisturbed system is asymptotically stable, so the problem can be reduced to examining the stability of the filter used in the control law. Both filters can be considered stable filters as they are strictly proper, bounded-input bounded-output stable. In previous UDE works, the majority of discussion on stability stops upon showing that the disturbance estimation error given by

$$\tilde{\boldsymbol{d}} = \boldsymbol{d} - \boldsymbol{d}_e = (1 - \boldsymbol{G}_f(s))\boldsymbol{d} \tag{19}$$

$$\tilde{\boldsymbol{D}}(s) = (1 - \boldsymbol{G}_f(s))\boldsymbol{D}(s) = \boldsymbol{W}(s)\boldsymbol{D}(s) \tag{20}$$

converges to zero when a low-pass filter with a high enough cutoff frequency is selected. While a similar analysis can be performed for the novel filter, it does not adequately show the effect of the novel targeted filtering structure.

Two measures are used to compare efficacy of the filters: the expected disturbance estimation error $\tilde{\boldsymbol{D}}(s)$ and the expected state tracking error $\boldsymbol{X}(s)$. These quantities are modelled by eqs. (20) and (16), where the impact of the disturbance $\boldsymbol{D}(s)$ on $\tilde{\boldsymbol{D}}(s)$ and $\boldsymbol{X}(s)$ is modelled by the transfer functions $\boldsymbol{W}(s)$ and $\boldsymbol{Z}(s)$. By examining the behaviour of these transfer functions, the difference between the novel filter and the standard low-pass filter can be more clearly quantified.

The Bode magnitude plot for $\boldsymbol{W}(s)$ is given in Fig. 3. From (20), it can be seen that it is desirable to have $\boldsymbol{W}(s)$ minimized, particularly at frequencies where the $\boldsymbol{D}(s)$ is non-zero. In the case of disturbance estimation error, the novel filter outperforms the standard filter across all frequencies, where $\boldsymbol{W}(s)$ for the novel filter has significantly lower gain and thus increased attenuation of the input signal $\boldsymbol{D}(s)$. A similar plot with similar results is produced for $\boldsymbol{Z}(s)$ in Fig. 4, though the result is based on the singular values of $\boldsymbol{Z}(s)$, which is now MIMO due to the incorporation of the linear aircraft model in the transfer function. With

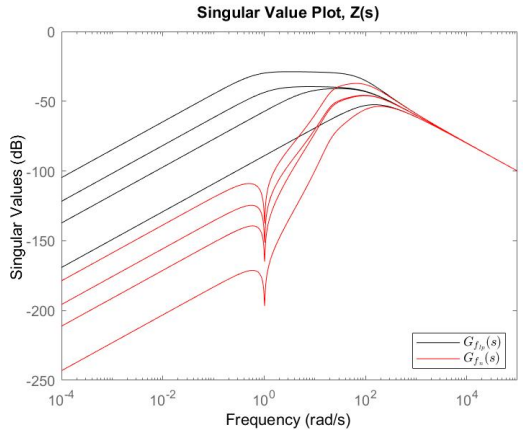

Fig. 4. Singular value plot of the transfer function $\boldsymbol{Z}(s)$, with the standard UDE low-pass filter (black) and the novel proposed filter (red).

both transfer functions, the difference in gain was designed to be largest in the frequency range where $\boldsymbol{D}(s)$ is most significant, as identified from spectral analysis of the state signals.

IV. Results

Verification of the proposed control law was done using MATLAB/Simulink. An XR-61T aerobatic vehicle was modelled and represented using the dynamic equations described in Section II, and two test cases were used to examine the difference between the different UDE filtering structures: first, steady-level flight transitioning to the harrier maneuver, and second, stabilization of the harrier maneuver from a slightly perturbed state.

The control law (15) has very similar performance when transitioning from steady level flight to the harrier maneuver when using either the standard low-pass filter (17) or the targeted filter (18), though there is some small difference in the tracking errors at steady state. However, when maintaining the harrier maneuver, it can be observed how the novel filter settles better than the standard low-pass filter. This result

is consistent with the expectations from the error dynamics, where near-constant disturbances experience strong attenuation from both filters, but time-varying disturbances close to the target frequency of 1 rad/s are filtered more strongly by the novel filter.

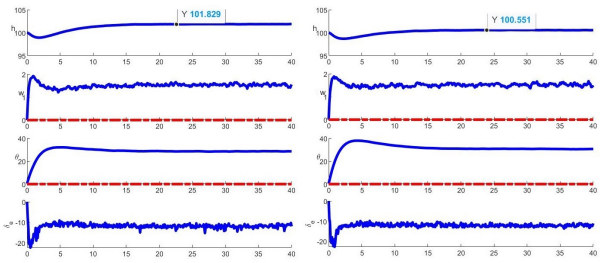

Fig. 5. Comparison of altitude tracking problem during steady-level to harrier maneuver, with the standard UDE low-pass filter $\omega_{lp} = 100$ rad/s (left) and the novel proposed filter (right).

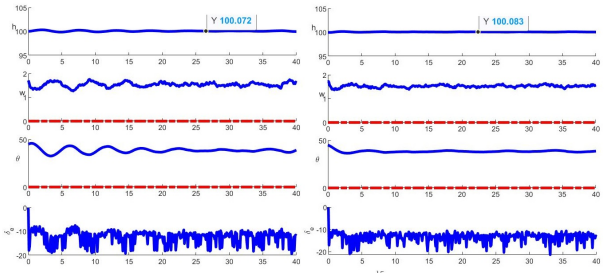

Fig. 6. Comparison of altitude tracking problem while maintaining harrier maneuver, with the standard UDE low-pass filter $\omega_{lp} = 100$ rad/s (left) and the novel proposed filter (right).

V. Conclusion

In this paper, a novel UDE controller using targeted filtering was proposed as improvement compared to typical UDE controllers, and was verified on a vehicle performing a simulated harrier maneuver. Overall, though method shows promise, the efficacy of using targeted filtering depends on the identification of the disturbance signal frequency content and a suitable filter structure to minimize tracking error based on the error dynamics of the system. If these can be achieved, then the targeted filtering structure can be shown to attenuate disturbance effects more strongly than conventional UDE.

References

[1] A. Frank, J. McGrew, M. Valenti, D. Levine, and J. How, "Hover, Transition, and Level Flight Control Design for a Single-Propeller Indoor Airplane," in *AIAA Guidance, Navigation and Control Conference and Exhibit*, Aug 2007.

[2] R. Cory and R. Tedrake, "Experiments in Fixed-Wing UAV Perching," in *AIAA Guidance, Navigation and Control Conf. and Exhibit*, Aug 2008.

[3] F. Sobolic, "Agile flight control techniques for a fixed-wing aircraft," Ph.D. dissertation, Dept. of Aeronautics and Astronautics, Massachusetts Institute of Technology, Cambridge, MA, USA, 2009.

[4] S. Park, "Autonomous aerobatics on commanded path," *Aerospace Science and Technology*, vol. 22, no. 1, pp. 64–74, oct 2012.

[5] E. Bulka, "Control and Obstacle Avoidance for Agile Fixed-Wing Aircraft," Ph.D. dissertation, Dept. of Mechanical Engineering, McGill University, 2021.

[6] J. C. H. Ramirez and M. Nahon, "Pilot-Assist Landing System for Hover-Capable Fixed-Wing Unmanned Aerial Vehicles in All Flight Regimes," *2021 International Conference on Unmanned Aircraft Systems, ICUAS 2021*, pp. 1179–1186, 2021.

[7] E. Bulka and M. Nahon, "High-Speed Obstacle-Avoidance with Agile Fixed-Wing Aircraft," in *2019 International Conference on Unmanned Aircraft Systems (ICUAS)*, 2019, pp. 971–980.

[8] W. Khan, "Dynamics Modeling of Agile Fixed-Wing Unmanned Aerial Vehicles," Ph.D. dissertation, Dept. of Mechanical Eng., McGill University, Montreal, QB, Canada, 2016.

[9] M. Selig, "Modeling Propeller Aerodynamics and Slipstream Effects on Small UAVs in Realtime," in *AIAA Atmospheric Flight Mechanics Conference*, ser. Guidance, Navigation, and Control and Co-located Conferences, Toronto, ON, Canada, Aug 2010.

[10] B. Johnson and R. Lind, "High Angle-of-Attack Flight Dynamics of Small UAVs," in *47th AIAA Aerospace Sciences Meeting*, ser. Aerospace Sciences Meetings, Orlando, FL, USA, Jan 2009.

[11] M. Goman and A. Khrabrov, "State-space representation of aerodynamic characteristics of an aircraft at high angles of attack," *Journal of Aircraft*, vol. 31, no. 5, pp. 1109–1115, sep 1994.

[12] S. Gill, M. Lowenberg, S. Neild, L. Crespo, B. Krauskopf, and G. Puyou, "Nonlinear Dynamics of Aircraft Controller Characteristics Outside the Standard Flight Envelope," *Journal of Guidance, Control, and Dynamics*, vol. 38, no. 12, pp. 2301–2308, mar 2015.

[13] Q. C. Zhong and D. Rees, "Control of uncertain LTI systems based on an uncertainty and disturbance estimator," *Journal of Dynamic Systems, Measurement and Control, Transactions of the ASME*, vol. 126, no. 4, pp. 905–910, 2004.

[14] Q. Zhang and H. H. T. Liu, "Aerodynamic model-based robust adaptive control for close formation flight," *Aerospace Science and Technology*, vol. 79, pp. 5–16, 2018.

[15] A. Kuperman and Q. Zhong, "UDE-based linear robust control for a class of nonlinear systems with application to wing rock motion stabilization," *Nonlinear Dynamics*, vol. 81, no. 1-2, pp. 789–799, 2015.

[16] Z. Yin, W. He, O. Kaynak, C. Yang, L. Cheng, and Y. Wang, "Uncertainty and Disturbance Estimator-Based Control of a Flapping-Wing Aerial Vehicle with Unknown Backlash-Like Hysteresis," *IEEE Trans. on Industrial Electronics*, vol. 67, no. 6, pp. 4826–4835, 2020.

[17] X. Zhang, H. Li, B. Zhu, and Y. Zhu, "Improved UDE and LSO for a class of uncertain second-order nonlinear systems without velocity measurements," *IEEE Transactions on Instrumentation and Measurement*, vol. 69, no. 7, pp. 4076–4092, 2020.

[18] R. Beard and T. McLain, *Small Unmanned Aircraft: Theory and Practice*. Princeton University Press, 2012.

[19] W. F. Phillips and D. O. Snyder, "Modern adaptation of prandtl's classic lifting-line theory," *Journal of Aircraft*, vol. 37, no. 4, pp. 662–670, 2000.

[20] D. Hunsaker, "Post Stall Behavior of a Lifting Line Algorithm," no. November, pp. 1–7, 2007.

[21] B. Montgomerie, "Methods for Root Effects, Tip Effects and Extending the ANgle of Attack Range to +- 180, with application to Aerodynamics for Blades on Wind Turbines and Propellers.pdf," no. June, p. 53, 2004.

[22] M. Selig, "Modeling Propeller Aerodynamics and Slipstream Effects on Small UAVs in Realtime," in *AIAA Atmospheric Flight Mechanics Conference*, Aug 2010.

[23] B. W. McCormick, *Aerodynamics, Aeronautics, and Flight Mechanics*. John Wiley & Sons, 1995.

[24] M. J. Dillsaver, "Gust Response and Control of Very Flexible Aircraft," Ph.D. dissertation, Dept. of Aerospace Engineering, University of Michigan, 2013.

[25] T. Colonius and D. R. Williams, "Control of vortex shedding on two- and three-dimensional airfoils," *Phil. Trans. R. Soc.*, pp. 1–15, 2008.

[26] K. E. Swalwell, J. Sheridan, and W. H. Melbourne, "Frequency analysis of surface pressures on an airfoil after stall," *21st AIAA Applied Aerodynamics Conference*, pp. 1–8, 2003.

[27] S. Yarusevych, P. E. Sullivan, and J. G. Kawall, "On vortex shedding from an airfoil in low-Reynolds-number flows," *Journal of Fluid Mechanics*, vol. 632, no. January, pp. 245–271, 2009.